1-1-2012

Probing exchange bias effects in CoO/Co Bilayers with Pillar-Like CoO structures

David Laurence Cortie
University of Wollongong, dlc422@uowmail.edu.au

Chin Shueh
National Chung Hsing University, Taiwan

Pei-Shi Chen
National Chung Hsing University, Taiwan

Jian-Fa Gao
National Chung Hsing University, Taiwan

Frank Klose
ANSTO, Frank.Klose@ansto.gov.au

See next page for additional authors

Japanese Journal of Applied Physics **51** (2012) 11PG01 **REGULAR PAPER**
http://dx.doi.org/**10.1143/JJAP.51.11PG01**

Probing Exchange Bias Effects in CoO/Co Bilayers with Pillar-Like CoO Structures

David Laurence Cortie[1,2], Chin Shueh[3], Pei-shi Chen[3], Jian-Fa Gao[3], Frank Klose[2], Jan van Lierop[4], and Ko-Wei Lin[3*]

[1]*The Institute for Superconducting and Electronic Materials, The University of Wollongong, Wollongong, NSW 2522, Australia*
[2]*The Australian Nuclear Science and Technology Organization, Kirrawee, NSW 2232, Australia*
[3]*Department of Materials Science and Engineering, National Chung Hsing University, Taichung 402, Taiwan*
[4]*Department of Physics and Astronomy, University of Manitoba, Winnipeg, R3T 2N2, Canada*

Received June 1, 2012; revised August 6, 2012; accepted August 16, 2012; published online November 20, 2012

Exchange bias effects in CoO/Co bilayers fabricated by ion-assisted deposition were studied as a function of CoO thickness. During the deposition of the top CoO layer, pillar-like CoO structures were embedded in the underlying Co layer due to implantation of oxygen ions. The enhanced coercivity was attributed to the changes in the magnetic reversal mechanism in the ferromagnetic Co layer due to the penetration of pillar-like structures of antiferromagnetic CoO. At low temperature, we found a strong exchange bias field. Our measurements indicate that the exchange bias effect can exist in a nanocomposite system that has a disordered mixture of columnar and planar Co/CoO interfaces.

1. Introduction

Within the models of magnetic exchange bias for an idealized ferromagnet/antiferromagnetic thin film, the hysteresis shift should be identical regardless of whether the ferromagnet is deposited on-top of the antiferromagnet or *vice versa*.[1,2] However, for thin film systems fabricated using sputtering deposition techniques, the exchange bias is often different for the two cases[3,4] because imperfections in the film microstructure, such as interface morphology, can depend closely on the growth sequence. In past work, when we studied the exchange bias effects in antiferromagnetic/ferromagnetic (AFM/FM) bilayers [such as in NiFe/CoO,[5] NiCo/(Ni,Co)O[6]] we deposited the ferromagnet on-top of the underlying antiferromagnetic oxide using ion-assisted deposition. However, in this study we investigate the oxygen ion-beam assisted growth of antiferromagnetic CoO layers on-top of a ferromagnetic cobalt layer to explore the impact of the oxygen-bombardment on the underlying FM film. It is found that during the fabrication of the top CoO layer, pillar-like CoO structures were formed near the interface due to the penetration of oxygen into the bottom Co layer. We studied this effect as a function of the CoO film layer thickness. We find that these pillar-like CoO structures at the interface between the Co and the CoO layers strongly affect the magnetic reversal process in these films.

2. Experimental Methods

A dual ion-beam deposition technique[5,6] was used to prepare the CoO/Co bilayers on SiO_2 substrates. A series of samples was deposited where the underlying Co layer thickness was kept constant at 65 nm, while the upper CoO layer was varied from 20 to 170 nm. A Kaufman ion source (800 V, 7.5 mA) was used to focus an argon ion-beam onto a commercial Co target surface while the End–Hall source ($V_{EH} = 100$ V, 500 mA) was used to *in-situ* bombard the growing film during CoO layer deposition with a mixture of 15% O_2/Ar. No external magnetic field was applied during deposition. A JEOL [JEM-2010] transmission electron microscope (TEM) operating at 200 kV was used for the microstructural analysis. Magnetic measurements were performed in a commercial vibrating sample magnetometer (DMS VSM). Field-cooling was performed by initially applying a +10 kOe field at 350 K to saturate the sample, before applying either ±1000 Oe field while cooling to 200 K. In these measurements, the exchange bias field, H_{ex}, was defined as the shift of the hysteresis loop along the field axis with respect to zero, $H_{ex} = (H_{c1} + H_{c2})/2$, where H_{c1} and H_{c2} are the negative and positive field coercivity, respectively.

3. Results

Figure 1 shows the structures of the CoO/Co bilayers characterized by TEM. The bottom Co and top CoO layer consist of hcp. Co ($a \sim 2.53$ Å, $c \sim 4.26$ Å) and rock-salt CoO ($a = 4.25$ Å), respectively. The grain sizes range from 5 to 15 nm, as shown in Figs. 1(a) and 1(b). The CoO lattice constant does not show any dependency on the overall CoO layer thickness (20–170 nm), and all films exhibit the same lattice constant determined from the electron diffraction patterns, shown in the inset of Fig. 1(c). This result shows that the oxygen stoichiometry and film strain for the CoO layer was essentially constant for the entire series. The morphology of CoO (50 nm)/Co (65 nm)/SiO_2 bilayer is shown by the cross-sectional TEM image in Fig. 1(d). The high-resolution TEM clearly shows that the interface between the Co and the CoO layer is diffuse, with a high degree of intermixing. A fraction of the CoO phase penetrates deep into the Co layer in the form of pillar-like structures. The diffusion depth of the oxygen atoms is estimated to be about half of the nominal Co layer thickness (30–35 nm). The presence of an oxygen gradient within the cobalt layer was qualitatively confirmed using energy dispersive X-ray (EDX) mapping. At the ion-energies used (0.13 keV), the penetration of oxygen ions into the underlying layer should only be 4–7 Å according to Monte Carlo simulations using the TRIM software package for oxygen implantation into cobalt with mass density 8.8 g/cm.[7] Thus, it is most likely that the pillar-like CoO structures are formed via subsequent grain-boundary diffusion of oxygen that was initially implanted in the near-surface region. From previous studies, it is expected that such irregular columnar structures of CoO will act as domain-pinning defects to alter the usual magnetic properties in these CoO/Co bilayers, as well as changing the dipolar interactions between cobalt-rich columns,[8] modulating the local Néel temperature[9] or introducing disordered crystal fields.[10]

Figure 2(a) shows the room temperature hysteresis loops of CoO/Co (65 nm)/SiO_2 bilayers with different CoO

*E-mail address: kwlin@dragon.nchu.edu.tw

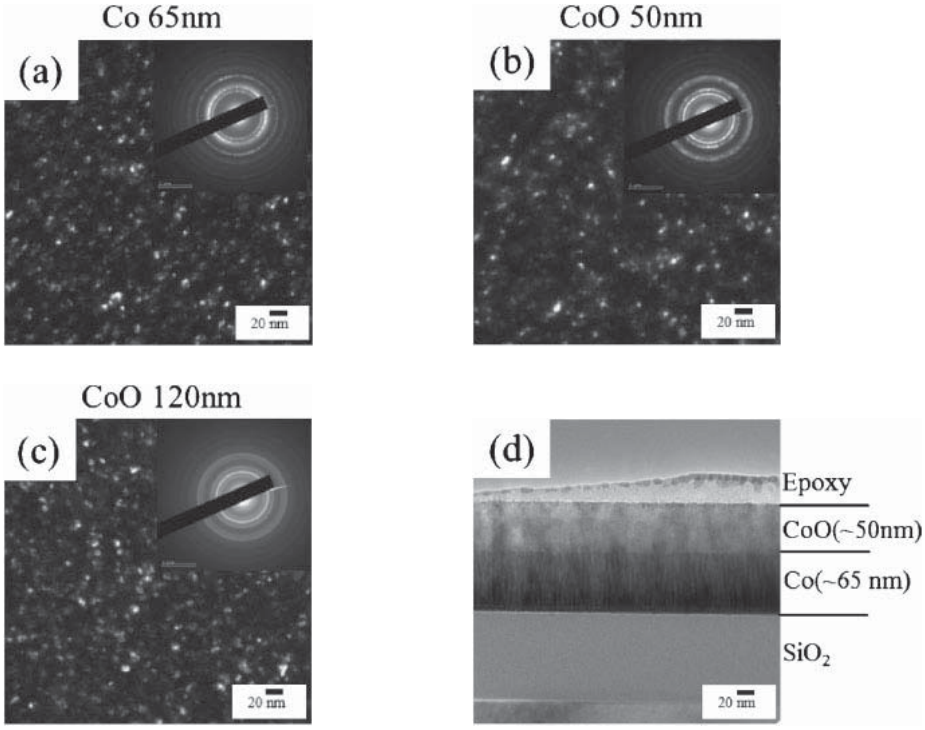

Fig. 1. The planar-view TEM micrographs of (a) the top Co layer (65 nm), (b) the bottom CoO layer (50 nm), and (c) CoO layer (120 nm). The electron diffraction patterns are shown in the inset of each figure. (d) The cross-sectional TEM micrograph illustrating the ion-beam bombardment effect (pillar-like CoO structures penetrating and embedded in the Co layer) on the $t_{CoO} = 50$ nm sample.

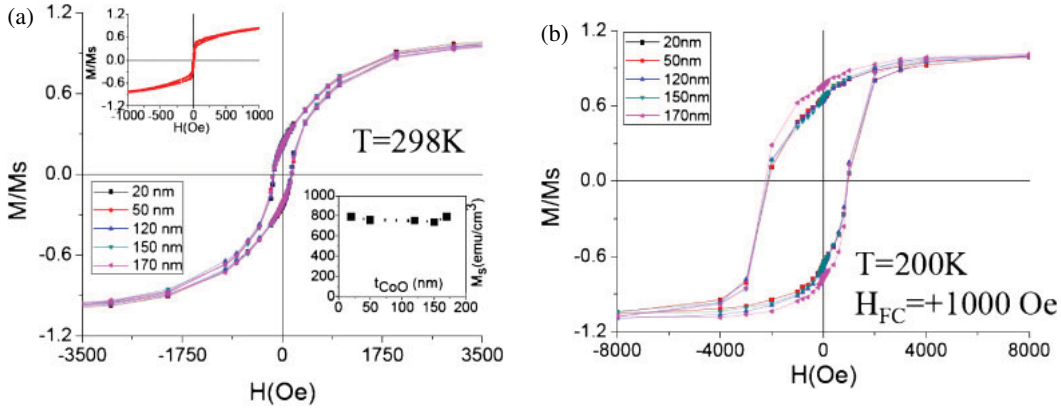

Fig. 2. (Color online) (a) The room temperature hysteresis loops of CoO/Co bilayers with different CoO layer thicknesses ($t = 20$ to 170 nm). The inset at top left shows the hysteresis loop of the reference single Co layer while the inset at bottom right shows the saturation magnetization of the Co layer with reduced M_s relative to the starting 65 nm Co volume owing to ion-beam bombardment effects. (b) The hysteresis loops of CoO ($t = 20$–170 nm)/Co bilayers measured at 200 K under field-cooling of +1000 Oe from 300 to 200 K.

thicknesses (20–170 nm). An enhanced coercivity (~150 Oe) was found in all of the bilayers compared to a reference pure Co layer [inset of Fig. 2(a), $H_c \sim 8$ Oe]. In addition to this, the average maximum magnetization of the bilayer film was reduced to approximately 455 emu/cm^3 for the 115-nm-thick film. If the volume of metallic cobalt in the original 65 nm region were preserved in a ferromagnetic, metallic state throughout deposition, one would expect a magnetization value of ~730 emu/cm^3 for the 115-nm-thick film. This is calculated by assuming that the volume fraction of cobalt versus cobalt oxide would be ~(65 nm/50 nm), and using the bulk cobalt magnetic saturation values of ~1300 emu/cm^3, and ~0 emu/cm^3 for the FM Co and AFM CoO, respectively.[11] Therefore the reduction in overall magnetization suggests that volume of magnetic cobalt was reduced by 46% from the nominal volume, which agrees adequately with the TEM result that shows the first ~30 nm of the original 65 nm contain a mixture of pillar-like structures which are predominantly CoO interspaced with smaller regions of metallic cobalt, reducing the overall cobalt metal volume fraction. Both the coercivity enhancement and lower magnetic saturation in the film series are attributed to the penetration of oxygen into the cobalt, and the formation of pillar-like CoO structures embedded within

the Co layer. The penetrating CoO regions are antiferromagnetic, and lower the average magnetization whilst also altering the magnetic reversal process of the neighboring cobalt by acting as defect sites and changing the magnetostatic energy landscape.[9,12] To first approximation, the average magnetic saturation per nominal 65-nm-thick Co volume is constant ($\sim$800 emu/cm^3) for all the films with different CoO layer-thicknesses as shown in the inset of Fig. 2(a). This result can be explained if the assumption is made that significant oxygen implantation into the Co only occurred during the growth of the first few monolayers of the CoO and stopped once the growing CoO exceeded a critical thickness, so that oxidization of the underlying cobalt layer was nearly equal in all cases, regardless of the final CoO thickness. The Néel temperature of CoO ($\sim$290 K in the bulk)[13] is below room temperature (298 K) and for this reason, no exchange bias is measured in the room temperature loops. Nonetheless it is possible that the coercivity enhancement observed at room temperature is the direct result of FM/AFM coupling, even though no exchange bias is observed, since this may be possible if the interfacial CoO moments have a locally enhanced T_N as proposed for NiFe/CoO[8] but are unstable against superparamagnetic activation. It is also possible that the coercivity enhancement originates from a distinct mechanism associated with altered shape-anisotropy from the dipolar interactions between ferromagnetic columns.[9,12] In either case, the unusual pillar-microstructure is seen to play a crucial role.

Upon field-cooling the CoO/Co bilayers in a positive field ($H_{FC} = +1000$ Oe) from 350 to 200 K (after first saturating the film in 10 kOe at 350 K), a clear exchange bias effect appears, accompanied by a pronounced asymmetry in the loop shape, as shown in Fig. 2(b). This indicates that exchange coupling between the Co FM and CoO AFM spin structures enables a loop-shift, despite the diffuse interface and unusual film morphology. Note that all of the magnetometry diagrams compare the loops of the first magnetic reversal for all samples in the untrained magnetic state.

To further understand the role of the CoO layer thickness on the magnetic exchange coupling, different CoO thicknesses were studied. The dependence of the coercivity and the magnitude of exchange bias field ($|H_{ex}|$) on the top CoO layer thicknesses is presented in Fig. 3 for the cases where the film was cooled in either a $+1000$ or a -1000 Oe to 200 K. All of the CoO/Co bilayers show a 10-fold increase in coercivity, $H_c \sim 1500$ Oe at low temperature that does not depend strongly on the top CoO layer thickness, or the polarity of the cooling field. This enhancement suggests that the transition to an ordered antiferromagnetic state within the CoO regions affects the magnetic properties of the surrounding cobalt through the coupling of the two different magnetic species. The independence of the coercivity from CoO thickness at both temperatures suggests that the columnar interface region, rather than the bulk overlying CoO region, largely determines the exchange coupling of the thin film bilayers, since if this were not the case, one would expect a measurable dependence of H_c and H_{ex} on the overlying CoO thickness. Figure 3(b) depicts the variation in strength of the exchange bias field for the different CoO layer thickness.

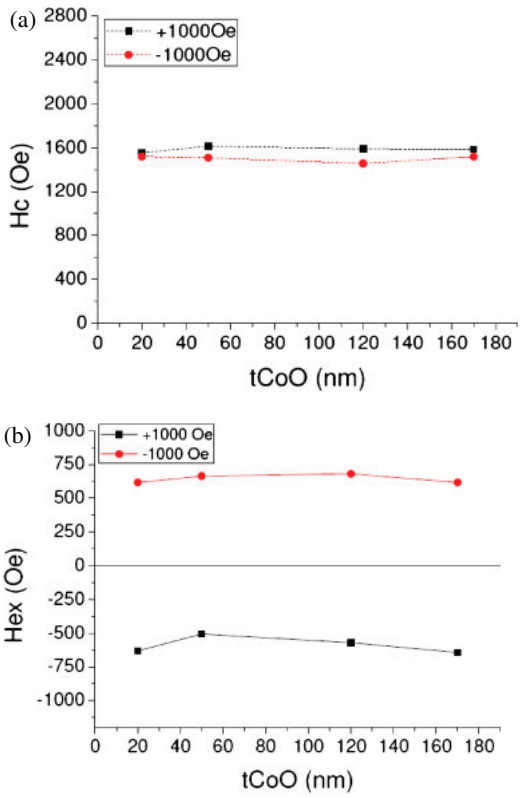

Fig. 3. (Color online) The CoO thickness dependence of (a) coercivity and (b) magnitude of exchange bias field in CoO/Co bilayers at 298 and 200 K after field cooling in $\pm$1000 Oe.

The presence of a strong exchange bias field, despite the highly diffuse, rough and disordered Co/CoO interface is noteworthy, since many models of exchange bias usually consider a planar interface with only a few monolayers of interfacial roughness.[2,13] In fact, the magnitude of the coercivity enhancement and exchange bias in the disordered nanocomposite Co/CoO at 200 K appears to be higher than that reported for epitaxial thin films with similar blocking and measurement temperatures and nearly perfect interfaces.[14] This striking result suggests that pillar-like antiferromagnetic in-growths into the ferromagnet, along with an mixed array of disordered interfaces, can in-fact enhance the measured exchange bias effect, in qualitative agreement with the anomalously large natural exchange bias observed in $Fe_2O_3/FeTiO_3$ ores with a mixed microstructure.[15] Figure 3(b) illustrates that the two different field-cooling configurations gave nearly equal exchange bias magnitudes. This is typical exchange bias behavior, and suggests that, despite the unusual film morphology, the 1000 Oe cooling-field was sufficient to eradicate any magnetic memory effects and enforce a well-defined in-plane magnetization direction during cooling.

It is known that the degree of the exchange interaction between FM and AFM layers can be estimated using the interfacial energy ($E_{int} = H_{ex} M_s t_{FM}$ erg/cm^2).[16] To compare the relative strength of exchange bias effects of CoO/Co bilayers for different AF thicknesses, the interfacial energy is calculated for the films series. Figure 4 presents this calculation using the ferromagnetic thicknesses estimated from the TEM cross sections and corresponding Co magnetization (M_s) estimated from the magnetometry. The

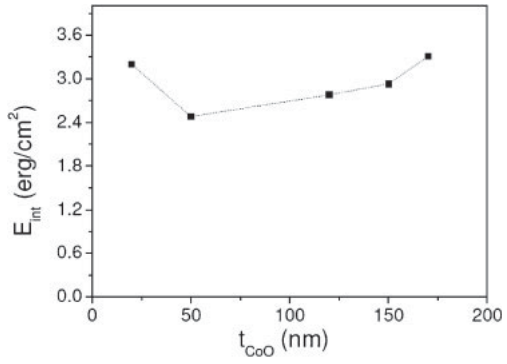

Fig. 4. The interfacial energy (E_{int}) as a function of CoO thicknesses in CoO/Co bilayers at 200 K after field cooling in +1000 Oe from 350 K.

interfacial energy product E_{int} for the mixed-interface film lies in the range 2.9–3.2 erg/cm^2 for all CoO thicknesses which is significantly higher compared with the interfacial energy for conventional Co/CoO bilayers that lie in the range ($E_{int} \sim 0.1$–0.8 erg/cm^2) for similar blocking temperatures.[13)]

4. Discussion and Conclusions

Despite the unusual interface morphology of disordered interpenetrating metal/metal–oxide pillars, the CoO/Co composite films studied here possess a remarkably strong exchange bias. Although Co/CoO is the oldest known exchange bias system,[17)] the past decade has revealed numerous new aspects regarding the advantageous role of structural disorder on the exchange bias at Co/CoO interfaces.[18–24)] In pioneering work, it was shown that the deliberate introduction of non-magnetic structural-defects into highly-crystalline epitaxial thin films of Co/CoO via dilution of the antiferromagnet with non-magnetic atoms such as Zn,[20)] or by deliberate crystal twinning,[21)] enhanced exchange bias by assisting the formation of dilute-antiferromagnetic thermal remnant magnetization,[22,23)] in accordance with the predictions of the atomistic domain state model (DSM).[24,25)] It is worth noting that in that body of work, the absolute maximum exchange bias recorded for such MBE-grown ~20 nm thick Co/CoO films was 700 Oe at 5 K,[21)] whereas all of our thicker ~60 nm sputtered films have a comparable exchange bias at 200 K, suggesting a higher blocking temperature and interfacial energy. The exchange bias found for the samples studied in this work is similar to the result found for epitaxial films Co where deliberate oxygen ion-implantation was performed to form Co/CoO nanocomposites ($H_{ex} \sim 400$ Oe), although there higher ion-beam energies were used (60 keV) presumably resulting in a different overall microstructure.[26)] The magnetic bias found in such nanocomposites is not altogether surprising, since a disordered oxide–metal interface could play a similar role to the defects in a diluted antiferromagnet[1)] or create random interfacial fields in the closely-related Malozemoff model.[27)] Additionally, oxide-pillars could act as pinning sights for Co ferromagnetic domain wall motion; provide a larger surface area for ferromagnetic/antiferromagnetic spin interactions and change the effective magnetostatic anisotropy.[12)] Despite the appearance of a mixture of columnar and planar interfaces in our samples, the strong exchange bias field was largely independent from the top CoO layer thicknesses. This implies that the interfacial region dominates the magnetic properties for the thickness regime studied. Collectively these results show the importance of carefully characterizing the microstructure and magnetic properties of an exchange-biased system to correctly understand the effect of deposition sequence on the resulting bilayer. Despite the inherent disorder of the Co/CoO interface, this work also shows that the deliberate formation of nanocomposite oxide regions within the Co layer can have certain technological advantages since both enhanced room-temperature coercivity and low-temperature exchange bias coexist.

Acknowledgments

This work was supported by the NSC of Taiwan and NSERC of Canada. David Cortie acknowledges the support of ANSTO and the Australian Institute of Nuclear Science and Engineering (AINSE).

1) U. Nowak, K. D. Usadel, J. Keller, P. Miltényi, B. Beschoten, and G. Güntherodt: Phys. Rev. B **66** (2002) 014430.
2) K. D. Usadel and R. L. Stamps: Phys. Rev. B **82** (2010) 094432.
3) T. Ambrose and C. L. Chien: Appl. Phys. Lett. **65** (1994) 1967.
4) E. V. Khomenko, N. G. Chechenin, I. O. Dzhun, N. S. Perov, V. V. Samsonova, A. Y. Goikhman, and A. V. Zenkevich: Phys. Solid State **52** (2010) 1701.
5) K.-W. Lin, F.-T. Lin, Y.-M. Tzeng, and Z.-Y. Guo: Eur. Phys. J. B **45** (2005) 237.
6) K.-W. Lin, J.-Y. Guo, H.-Y. Liu, H. Ouyang, Y.-L. Chan, D.-H. Wei, and J. v. Lierop: J. Appl. Phys. **103** (2008) 07C105.
7) J. P. Biersack and L. G. Haggmark: Nucl. Instrum. Methods **174** (1980) 257.
8) J. van Lierop, B. W. Southern, K.-W. Lin, Z.-Y. Guo, C. L. Harland, R. A. Rosenberg, and J. W. Freeland: Phys. Rev. B **76** (2007) 224432.
9) T. Iwata, R. J. Prosen, and B. E. Gran: J. Appl. Phys. **37** (1966) 1285.
10) V. I. Nikitenko, V. S. Gornakov, L. M. Dedukh, Y. P. Kabanov, A. F. Khapikov, A. J. Shapiro, R. D. Shull, A. Chaiken, and R. P. Michel: Phys. Rev. B **57** (1998) R8111.
11) J. García-Torres, E. Gomez, and E. Vallez: J. Appl. Electrochem. **39** (2009) 233.
12) K. Yoshida and T. Takayama: J. Magn. Magn. Mater. **82** (1989) 228.
13) J. Nogués and I. K. Schuller: J. Magn. Magn. Mater. **192** (1999) 203.
14) F. Radu, M. Etzkorn, R. Siebrecht, T. Schmitte, K. Westerholt, and H. Zabel: Phys. Rev. B **67** (2003) 134409.
15) S. A. McEnroe, B. Carter-Stiglitz, R. J. Harrison, P. Robinson, K. Fabian, and C. McCammon: Nat. Nanotechnol. **2** (2007) 631.
16) Y.-T. Chen: Nanoscale Res. Lett. **4** (2009) 90.
17) W. H. Meiklejohn and C. P. Bean: Phys. Rev. **102** (1956) 1413.
18) M. Gruyters and D. Riegel: Phys. Rev. B **63** (2000) 052401.
19) S. Brems, K. Temst, and C. V. Haesendonck: Phys. Rev. Lett. **99** (2007) 067201.
20) J. Keller, P. Miltényi, B. Beschoten, G. Güntherodt, U. Nowak, and K. D. Usadel: Phys. Rev. B **66** (2002) 014431.
21) M. R. Ghadimi, B. Beschoten, and G. Güntherodt: Appl. Phys. Lett. **87** (2005) 261903.
22) D. L. Cortie and J. Pillans: J. Comput. Sci. **2** (2011) 279.
23) S. R. Ali, M. R. Ghadimi, M. Fecioru-Morariu, B. Beschoten, and G. Güntherodt: Phys. Rev. B **85** (2012) 012404.
24) J.-I. Hong, T. Leo, D. J. Smith, and A. E. Berkowitz: Phys. Rev. Lett. **96** (2006) 117204.
25) P. Miltényi, M. Gierlings, J. Keller, B. Beschoten, and G. Güntherodt: Phys. Rev. Lett. **84** (2000) 4224.
26) J. Demeter, J. Meersschaut, F. Almeida, S. Brems, C. V. Haesendonck, A. Teichert, R. Steitz, K. Temst, and A. Vantomme: Appl. Phys. Lett. **96** (2010) 132503.
27) A. P. Malozemoff: Phys. Rev. B **35** (1987) 3679.